

UCSF

UC San Francisco Previously Published Works

Title

Simultaneous acquisition of T1ρ and T2 quantification in knee cartilage: Repeatability and diurnal variation

Permalink

<https://escholarship.org/uc/item/4qv2n1gp>

Journal

Journal of Magnetic Resonance Imaging, 39(5)

ISSN

1053-1807

Authors

Li, Xiaojuan

Wyatt, Cory

Rivoire, Julien

et al.

Publication Date

2014-05-01

DOI

10.1002/jmri.24253

Peer reviewed



Published in final edited form as:

J Magn Reson Imaging. 2014 May ; 39(5): 1287–1293. doi:10.1002/jmri.24253.

Simultaneous acquisition of T_{1ρ} and T₂ quantification in knee cartilage – reproducibility and diurnal variation

Xiaojuan Li, PhD¹, Cory Wyatt, PhD¹, Julien Rivoire, PhD¹, Eric Han, MS², Weitian Chen, PhD², Joseph Schooler, BS¹, Fei Liang, BS¹, Keerthi Shet, PhD¹, Richard Souza, PhD¹, and Sharmila Majumdar, PhD¹

¹Musculo-skeletal Quantitative Imaging Research (MQIR), Department of Radiology, University of California, San Francisco (UCSF), San Francisco, CA, USA

²Applied Science Laboratory (ASL), GE Healthcare, Menlo Park, CA, USA

Abstract

Purpose—To develop a robust sequence that combines T_{1ρ} and T₂ quantifications and to examine the *in-vivo* repeatability and diurnal variation of T_{1ρ} and T₂ quantifications in knee cartilage.

Materials and Methods—Six healthy volunteers were scanned in the morning and afternoon on two days using a combined T_{1ρ} and T₂ quantification sequence developed in this study. Repeatability of T_{1ρ} and T₂ quantification was estimated using root-mean-square coefficients-of-variation (RMS-CV). T_{1ρ} and T₂ values from morning scans were compared to those from afternoon scans using paired t-tests.

Results—The overall RMS-CV of *in-vivo* T_{1ρ} and T₂ quantification was 5.3% and 5.2% respectively. The RMS-CV of AM scans was 4.2% and 5.0% while the RMS-CV of PM scans was 6.0% and 6.3% for T_{1ρ} and T₂ respectively. No significant difference was found between T_{1ρ} or T₂ values in the morning and in the afternoon.

Conclusions—A sequence that combines T_{1ρ} and T₂ quantification with scan time less than 10 minutes and is robust to B₀ and B₁ inhomogeneity was developed with excellent repeatability. For a cohort with low-level daily activity, although no significant diurnal variation of cartilage MR relaxation times was observed, the afternoon scans had inferior repeatability compared to morning scans.

Keywords

Cartilage degeneration; T_{1ρ}; T₂; Repeatability; Diurnal variation

Introduction

Cartilage degeneration is a characteristic manifestation in pathologies such as osteoarthritis (OA). It is well established that biochemical changes of macromolecules within the cartilage matrix are among the initiating events of cartilage degeneration, and take place prior to morphologic changes of the tissue. Therefore, efforts have been made during the last decade on developing imaging techniques for cartilage matrix composition. Among the techniques developed, magnetic resonance (MR) T_{1ρ} and T₂ relaxation times have been proposed as promising imaging markers for early cartilage degeneration in OA (1, 2).

MR $T_{1\rho}$ and T_2 quantification in cartilage may provide complementary information associated with cartilage degeneration during OA due to their different relaxation mechanisms. In particular, while some studies show $T_{1\rho}$ is more sensitive than T_2 (which is more dominated by hydration and collagen changes) to proteoglycan loss in cartilage (3, 4), some others suggest both $T_{1\rho}$ and T_2 are sensitive to changes in proteoglycan contents in OA cartilage (5, 6). The sensitivity of $T_{1\rho}$ and T_2 to proteoglycan changes in cartilage matrix is still under investigation. However, studies investigating voxel-by-voxel relationship between $T_{1\rho}$ and T_2 are very limited (7). One difficulty is these two parameters are normally acquired with separate sequences and the correlation study may be sensitive to motion and potential variation caused by different sequence acquisition. It has been documented that T_2 quantifications were significantly different between using spin-echo, fast spin-echo (FSE), spoiled gradient echo (SPGR) and magnetization-prepared sequences (8). The T_2 values are also significantly higher when longer echo train length (ETLs) are used in FSE acquisitions (8). Furthermore, $T_{1\rho}$ and T_2 quantitative techniques normally need a long acquisition time because multiple $T_{1\rho}$ - or T_2 -weighted images need to be acquired to reconstruct the relaxation time map. Techniques towards shortening the overall acquisition time are desirable. A relatively short acquisition time (normally less than 10 minutes) is also critical to make these techniques feasible for clinical applications.

A couple of previous studies examined the diurnal variation in cartilage morphology (thickness and volume) in the knee joint (9, 10). However, no study has been documented yet on the potential diurnal variation of relaxation times in knee cartilage. The goals of this study were therefore three folds: 1) To develop a robust sequence that combines $T_{1\rho}$ and T_2 quantification; 2) To examine the *in-vivo* repeatability of $T_{1\rho}$ and T_2 quantification; 3) To examine the potential diurnal variation of $T_{1\rho}$ and T_2 quantification in cartilage in young healthy adults.

Methods

Sequence development

The sequence was developed based on the MAPSS (magnetization-prepared angle-modulated partitioned k-space spoiled gradient echo snapshots) $T_{1\rho}$ quantification sequence developed previously (11). The $T_{1\rho}$ preparation pulses contained continuous hard 90_x (tip down pulses) - spin lock pulses - 90_{-x} (tip up pulses). Multiple k-space lines (views per segmentation, VPS) are acquired immediately after each magnetization preparation. RF cycling was applied to eliminate the adverse impact of longitudinal relaxation on quantitative accuracy. This RF cycling scheme also yields a transient signal evolution that is independent of the prepared magnetization, and consequently a same variable flip angle train can be applied to provide a flat signal response to eliminate the filtering effect in k-space caused by transient signal evolution after each spin-lock (11). In this work, we added the following features to this sequence:

Improving the sequence robustness to B_1 and B_0 inhomogeneity—In the original MAPSS sequence, the phase of the second half of the spin-lock pulse was shifted 180° from the first half to reduce artifacts caused by B_1 inhomogeneity (12, 13). However, significant banding artifacts are often observed when there is B_0 inhomogeneity due to the off-axis rotation after the tip-down pulses. In this work, composite pulses, as originally proposed by Dixon et al. (14) were used. The tip-down/tip-up 90° hard pulses were followed and preceded by a hard 135° pulse with the opposite phase (Figure 1A). The composite tip down pulses will bring the magnetization near the spin-lock axis, and the composite tip up pulses bring the magnetization back near the longitudinal (z) axis even under the condition of a large off resonance (14).

Combining $T_{1\rho}$ and T_2 weighting—A combined $T_{1\rho}$ and T_2 sequence was designed containing an interchangeable preparation, in which either the $T_{1\rho}$ or the T_2 preparation could be run for any echo, and the $T_{1\rho}$ - and T_2 -weighted images will be acquired in one scan sequence. The T_2 preparation contained an MLEV (Malcolm Levitt's composite-pulse decoupling sequence) train of nonselective composite $90^\circ_x 180^\circ_y 90^\circ_x$ refocusing pulses (with the pulse duration of 1.624 ms) (15). In the case of the first TSL = 0 and first TE = 0, $T_{1\rho}$ and T_2 -weighted images share the first image.

Applying radial-centric view ordering to minimized eddy current effects—

Multiple k-space lines are acquired after each magnetization preparation, traversing in segmented radial-centric view ordering (16), as shown in Figure 1B, to minimize the eddy current effect (as compared to the segmented elliptic-centric order in the previous MAPSS sequence (11)).

The combined $T_{1\rho}/T_2$ sequence was validated in phantoms and control subjects by comparing the results to the published MAPSS sequence (11).

Subjects

Six healthy volunteers (age 22-35 years, 3 females) were recruited for this study. The scans were performed using a GE 3T scanner (Signa HDx, GE Healthcare, Milwaukee, WI) and an 8-channel phased array knee coil (Invivo, Gainesville, FL). Each subjects were scanned in the morning (between 8-10am) and in the afternoon (between 5-7pm), and scanned again on a second day after one week using the same protocol, resulting in four scans per subject (namely AM1, PM1, AM2, PM2). Each subject filled out modified International Physical Activity Questionnaires (IPAQ) for their activity levels for the past year (before AM1 scan), 1 week (before AM1 and AM2), and 1 day (before PM1 and PM2). The study was approved by the Committee for Human Research at our institution, and the informed consent was obtained from all subjects.

Imaging Protocols

The *in-vivo* imaging protocol included sagittal T_2 -weighted fat-saturated fast spin-echo (FSE) images (TR/TE = 4300/51 ms, FOV = 14 cm, matrix = 512×256 slice thickness = 2.5 mm, gap = 0.5 mm, echo train length (ETL) = 9, bandwidth = 31.25 kHz, NEX = 2), sagittal 3D fat-saturated high-resolution spoiled gradient-echo (SPGR) images (TR/TE = 15/6.7 ms, flip angle = 18, FOV = 14 cm, matrix = 512×512 , slice thickness = 1 mm, bandwidth = 31.25 kHz, NEX = 1), and the $T_{1\rho}/T_2$ quantification sequence (FOV = 14 cm, matrix = 256×128 , slice thickness = 4 mm, Views Per Segment = 64, time of recovery = 1.2 s, number of slices = 26; For $T_{1\rho}$: TSL = 0/10/40/80 ms, spin-lock frequency = 500 Hz; for T_2 : preparation TE = 0/13.7/27.3/54.7 ms; total acquisition time = 9 mins 30 sec). Parallel imaging ASSET (Array Spatial Sensitivity Encoding Technique) with acceleration factor (AF) as 2 was used for FSE and SPGR images. ARC (Autocalibrating Reconstruction for Cartesian imaging) parallel imaging with phase direction acceleration factor of 2 was used in $T_{1\rho}/T_2$ sequences. In each set of *in-vivo* scanning, phantoms with different concentrations (1% to 4%) of agarose were scanned with the $T_{1\rho}/T_2$ quantification sequences using the same parameters.

Image and Data Analysis

Cartilage of the lateral/medial femoral condyles (LFC/MFC), the lateral/medial tibia (LT/MT) and patella (P) were segmented semi-automatically in the SPGR images using in-house developed software (17). $T_{1\rho}$ and T_2 maps were reconstructed by fitting the $T_{1\rho}$ - and T_2 -weighted images voxel-by-voxel to the equations below:

$$S(TSL) \propto \exp(-TSL/T_{1\rho}) \quad [1]$$

$$S(TE) \propto \exp(-TE/T_2) \quad [2]$$

The images acquired in the combined $T_{1\rho}/T_2$ sequence with $TSL/TE = 0$ were rigidly registered to the high-resolution SPGR images, and the transformation matrix was applied to $T_{1\rho}$ and T_2 maps using the Visualization ToolKit Computational Imaging Science Group (VTK CISC) Registration Toolkit. The cartilage contours previously generated from SPGR images were overlaid on the registered $T_{1\rho}$ and T_2 maps, Figure 2. The mean and standard deviation of $T_{1\rho}$ and T_2 relaxation times were calculated in each defined compartments.

Statistical Analysis

Repeatability was estimated using root mean square coefficients of variation (RMS-CV). The $T_{1\rho}$ and T_2 values from morning scans were compared to the values from afternoon scans using a paired t-test and the significance level was 0.05. Diurnal variation was quantified as percentage change from morning to afternoon: $(PM-AM)/AM \times 100\%$.

Results

Comparison of the new sequence vs. MAPSS sequence

Figure 3 shows the images of phantoms and *in-vivo* knees using the original MAPSS sequence and the modified sequence. Significant banding artifact was observed at the edge of the phantom due to B_0 inhomogeneity, which was diminished using the composite tip-down/tip-up pulses (Figure 3A, 3B). The signal curve from the phantom showed non-exponential signal oscillation in the data without composite pulses, which introduced a poor fitting and an underestimate of $T_{1\rho}$ quantification; while the data using composite pulses had very good fitting of the exponential decay curve (Figure 3C). Figure 2D showed *in-vivo* $T_{1\rho}$ -weighted images that were acquired using the original MAPSS sequence in a healthy control and showed significant banding artifact due to B_0 inhomogeneity (Figure 3D). This banding artifact was significantly reduced when the composite pulses were applied for the tip-down/tip-up pulses (Figure 3E). Using images free of artifact from both sequences, the RMS-CV of quantified $T_{1\rho}$ and T_2 in phantoms between the new sequence and the previously published MAPSS sequence was 1.3% for $T_{1\rho}$ and 0.7% for T_2 , respectively. The RMS-CV of quantified $T_{1\rho}$ and T_2 *in-vivo* between the new sequence and the MAPSS sequence was 2.6% for $T_{1\rho}$ and 1.9% for T_2 , respectively.

Repeatability

Phantom Results—The RMS-CV of intra-day repeatability in phantoms was 1.0% for both $T_{1\rho}$ and T_2 quantification. The RMS-CV of inter-day repeatability in phantoms was 2.2% for $T_{1\rho}$ and 2.0% for T_2 , respectively.

In-vivo Repeatability—The overall RMS-CV of the scan-rescan quantification of $T_{1\rho}$ and T_2 was 5.3% and 5.2% respectively. When the data was separate for AM scans and PM scans, the RMS-CV of all AM scans was 4.2% and 5.0% for $T_{1\rho}$ and T_2 respectively, while the RMS-CV of all PM scans was 6.0% and 6.3% for $T_{1\rho}$ and T_2 respectively. The RMS-CV of each compartment ranged 2.2% - 5.9% for $T_{1\rho}$ AM, 4.8-8.8% for $T_{1\rho}$ PM, 4.0% - 6.2% for T_2 AM and 4.2% - 8.5% for T_2 PM, respectively, Figure 4.

Diurnal Variation

No significant difference was found in $T_{1\rho}$ or T_2 between the values obtained in the morning and in the afternoon in this cohort ($P > 0.05$ for both $T_{1\rho}$ and T_2). $T_{1\rho}$ and T_2 measured in AMs were significantly correlated with the measures in PMs ($R = 0.81$ and $R = 0.85$, $P < 0.01$). The change percentage from AM scans to PM scans ranged from -3.4% to 1.8% in the defined five compartments, with a large variation among each individual subjects (as indicated with large SD of the percentage change, Table 1).

Discussion

A 3D sequence that can simultaneously quantify $T_{1\rho}$ and T_2 relaxation times was developed. Concatenation of the two measurements in a single scan will allow direct (pixel-by-pixel) comparison between $T_{1\rho}$ and T_2 maps by removing potential quantification variations caused by different acquisition sequences (spin-echo vs gradient-echo sequences for example) and minimizing chances of motion between these two quantifications. The developed sequence combines $T_{1\rho}$ and T_2 quantification and the current study saves scan time compared to separate $T_{1\rho}$ and T_2 quantification sequences by sharing the TSL = 0 and TE = 0 image. Currently the total scan time is less than 10 minutes to obtain both quantifications, which will greatly facilitate potential clinical applications of these advanced MR techniques. Further, combining $T_{1\rho}$ and T_2 acquisition in one sequence will increase the parameter dimension and can potentially help with further acceleration using advanced techniques, which we will explore in the future.

In this work, the composite pulses originally proposed by Dixon et al. were used for tip-down and tip-up pulses during $T_{1\rho}$ and T_2 preparation. Chen et al. showed earlier that combining the composite pulses and RF-cycling can simultaneously correct B_0 magnetic field inhomogeneity effects and B_1 RF inhomogeneity effects (image artifact and $T_{2\rho}$ contamination) (18). Images from phantoms and *in-vivo* knees from this study confirmed that the modified sequence is robust for potential B_0 and B_1 inhomogeneity.

Our study showed that the developed sequence provided excellent *in-vivo* repeatability for $T_{1\rho}$ and T_2 quantification. The *in-vivo* inter-day repeatability is comparable to the previously published intra-day repeatability (5). However, the repeatability of the PM $T_{1\rho}$ and T_2 were inferior to the AM scans, which may potentially be due to the variation introduced by different activity levels during the day. Therefore, for large cohort and longitudinal studies, it may be optimal to scan subjects early in the morning to minimize potential variation in relaxation times caused by differences in activity levels and loadings during the day. An alternative strategy to minimize the loading effect is to equilibrate the loading condition right before the scan, by for example sitting in the wheel chair for more than 30 minutes.

No significant diurnal variation of cartilage MR relaxation times was found in this cohort. Previous study in young healthy volunteers ($n=6$ and 10 respectively) reported significant decrease cartilage thickness from mornings to evenings, especially in medial tibial and femoral condyle (9, 10). The subjects included in the study performed by Waterton et al. spent the day predominantly in the laboratory, mostly standing at a bench, which introduced quite different loading condition compared to subjects in our study. Our study cohort is composed with subjects who spent most of their day sitting (the hours for sitting ranged from 6-10 hours on the scan days based on the IPAQ questionnaires). This low level of daily activity may introduce very mild loading to the knee joint, therefore introduce minimal variation of the MR relaxation times.

Previous studies of vertebral discs demonstrated significant decrease in T_2 from mornings to evenings (19, 20) ($n = 6$ and 18 respectively), which can be explained by that the vertebral

discs normally experience continuous loading during the day. Interestingly, Karakida et al. showed that this significant decrease of disc T_2 was only observed in healthy normal discs before the age of 35 years, but not in normal discs after 35 years and in degenerated discs (20). This result suggested that the response of disc matrix to loading is affected by aging and degeneration. Future studies for diurnal variation of knee cartilage shall include subjects who spend more time standing or in other loading-inducing activities, and explore the potential relationship between degeneration and diurnal variation.

In conclusion, a sequence that combines $T_{1\rho}$ and T_2 quantification with a total scan time less than 10 minutes and is robust to B_0 and B_1 inhomogeneity was developed with excellent *in-vivo* repeatability. Such sequences have the great potential to be applied in future clinical trials and studies. For a cohort with relatively low level of daily activity, although no significant diurnal variation of cartilage MR relaxation times was observed, the scans in the afternoon had inferior repeatability compared to those in the morning.

References

1. Crema MD, Roemer FW, Marra MD, Burstein D, Gold GE, Eckstein F, et al. Articular cartilage in the knee: current MR imaging techniques and applications in clinical practice and research. *Radiographics*. 2011; 31(1):37–61. Epub 2011/01/25. 10.1148/rg.311105084 [PubMed: 21257932]
2. Li X, Ma C, Link T, Castillo D, Blumenkrantz G, Lozano J, et al. In vivo $T_{1\rho}$ and T_2 mapping of articular cartilage in osteoarthritis of the knee using 3 Tesla MRI. *Osteoarthritis and Cartilage*. 2007; 15(7):789–97. [PubMed: 17307365]
3. Regatte RR, Akella SV, Borthakur A, Kneeland JB, Reddy R. Proteoglycan depletion-induced changes in transverse relaxation maps of cartilage: comparison of T_2 and $T_{1\rho}$. *Acad Radiol*. 2002; 9(12):1388–94. [PubMed: 12553350]
4. Li X, Cheng J, Lin K, Saadat E, Bolbos RI, Jobke B, et al. Quantitative MRI using $T_{1\rho}$ and T_2 in human osteoarthritic cartilage specimens: correlation with biochemical measurements and histology. *Magn Reson Imaging*. 2011; 29(3):324–34. Epub 2010/12/07. doi: S0730-725X(10)00308-5 [pii] 10.1016/j.mri.2010.09.004. [PubMed: 21130590]
5. Keenan KE, Besier TF, Pauly JM, Han E, Rosenberg J, Smith RL, et al. Prediction of glycosaminoglycan content in human cartilage by age, $T_{1\rho}$ and T_2 MRI. *Osteoarthritis Cartilage*. 2011; 19(2):171–9. Epub 2010/11/30. 10.1016/j.joca.2010.11.009 [PubMed: 21112409]
6. Wong CS, Yan CH, Gong NJ, Li T, Chan Q, Chu YC. Imaging biomarker with $T_{1\rho}$ and T_2 mappings in osteoarthritis - In vivo human articular cartilage study. *Eur J Radiol*. 2013; 82(4):647–50. Epub 2013/01/22. 10.1016/j.ejrad.2012.11.036 [PubMed: 23333531]
7. Li X, Pai A, Blumenkrantz G, Carballido-Gamio J, Link T, Ma B, et al. Spatial distribution and relationship of $T_{1\rho}$ and T_2 relaxation times in knee cartilage with osteoarthritis. *Magn Reson Med*. 2009; 61(6):1310–8. Epub 2009/03/26. 10.1002/mrm.21877 [PubMed: 19319904]
8. Pai A, Li X, Majumdar S. A comparative study at 3 T of sequence dependence of T_2 quantitation in the knee. *Magn Reson Imaging*. 2008; 26(9):1215–20. [PubMed: 18502073]
9. Waterton JC, Solloway S, Foster JE, Keen MC, Gandy S, Middleton BJ, et al. Diurnal variation in the femoral articular cartilage of the knee in young adult humans. *Magn Reson Med*. 2000; 43(1):126–32. Epub 2000/01/22. doi: 10.1002/(SICI)1522-2594(200001)43:1<126::AID-MRM15>3.0.CO;2-# [pii]. [PubMed: 10642739]
10. Coleman JL, Widmyer MR, Leddy HA, Utturkar GM, Spritzer CE, Moorman CT 3rd, et al. Diurnal variations in articular cartilage thickness and strain in the human knee. *J Biomech*. 2012. Epub 2012/10/30. 10.1016/j.jbiomech.2012.09.013 [PubMed: 23102493]
11. Li X, Han E, Busse R, Majumdar S. In vivo $T_{1\rho}$ mapping in cartilage using 3D magnetization-prepared angle-modulated partitioned k-space spoiled gradient echo snapshots (3D MAPSS). *Magn Reson Med*. 2008; 59(2):298–307. [PubMed: 18228578]
12. Charagundla SR, Borthakur A, Leigh JS, Reddy R. Artifacts in $T_{1\rho}$ -weighted imaging: correction with a self-compensating spin-locking pulse. *J Magn Reson*. 2003; 162(1):113–21. [PubMed: 12762988]

13. Li X, Han E, Ma C, Link T, Newitt D, Majumdar S. In vivo 3T spiral imaging based multi-slice T(1rho) mapping of knee cartilage in osteoarthritis. *Magnetic resonance in medicine*. 2005; 54(4): 929–36. [PubMed: 16155867]
14. Dixon WT, Oshinski JN, Trudeau JD, Arnold BC, Pettigrew RI. Myocardial suppression in vivo by spin locking with composite pulses. *Magn Reson Med*. 1996; 36(1):90–4. [PubMed: 8795026]
15. Foltz W, Stainsby J, Wright G. T2 accuracy on a whole-body imager. *Magn Reson Med*. 1997; 38(5):759–68. [PubMed: 9358450]
16. Busse RF, Brau AC, Vu A, Michelich CR, Bayram E, Kijowski R, et al. Effects of refocusing flip angle modulation and view ordering in 3D fast spin echo. *Magn Reson Med*. 2008; 60(3):640–9. Epub 2008/08/30. 10.1002/mrm.21680 [PubMed: 18727082]
17. Carballido-Gamio J, Bauer JS, R S, Lee KY, Krause S, Link TM, et al. Inter-subject comparison of MRI knee cartilage thickness. *Medical Image Analysis*. 2007; 12(2):120–35. [PubMed: 17923429]
18. Chen W, Takahashi A, Han E. Quantitative T(1)(rho) imaging using phase cycling for B0 and B1 field inhomogeneity compensation. *Magn Reson Imaging*. 2011; 29(5):608–19. Epub 2011/04/29. doi: S0730-725X(11)00064-6 [pii] 10.1016/j.mri.2011.02.002. [PubMed: 21524869]
19. Ludescher B, Effelsberg J, Martirosian P, Steidle G, Markert B, Claussen C, et al. T2- and diffusion-maps reveal diurnal changes of intervertebral disc composition: an in vivo MRI study at 1.5 Tesla. *J Magn Reson Imaging*. 2008; 28(1):252–7. Epub 2008/06/27. 10.1002/jmri.21390 [PubMed: 18581387]
20. Karakida O, Ueda H, Ueda M, Miyasaka T. Diurnal T2 value changes in the lumbar intervertebral discs. *Clin Radiol*. 2003; 58(5):389–92. Epub 2003/05/03. doi: S0009926002005834 [pii]. [PubMed: 12727168]

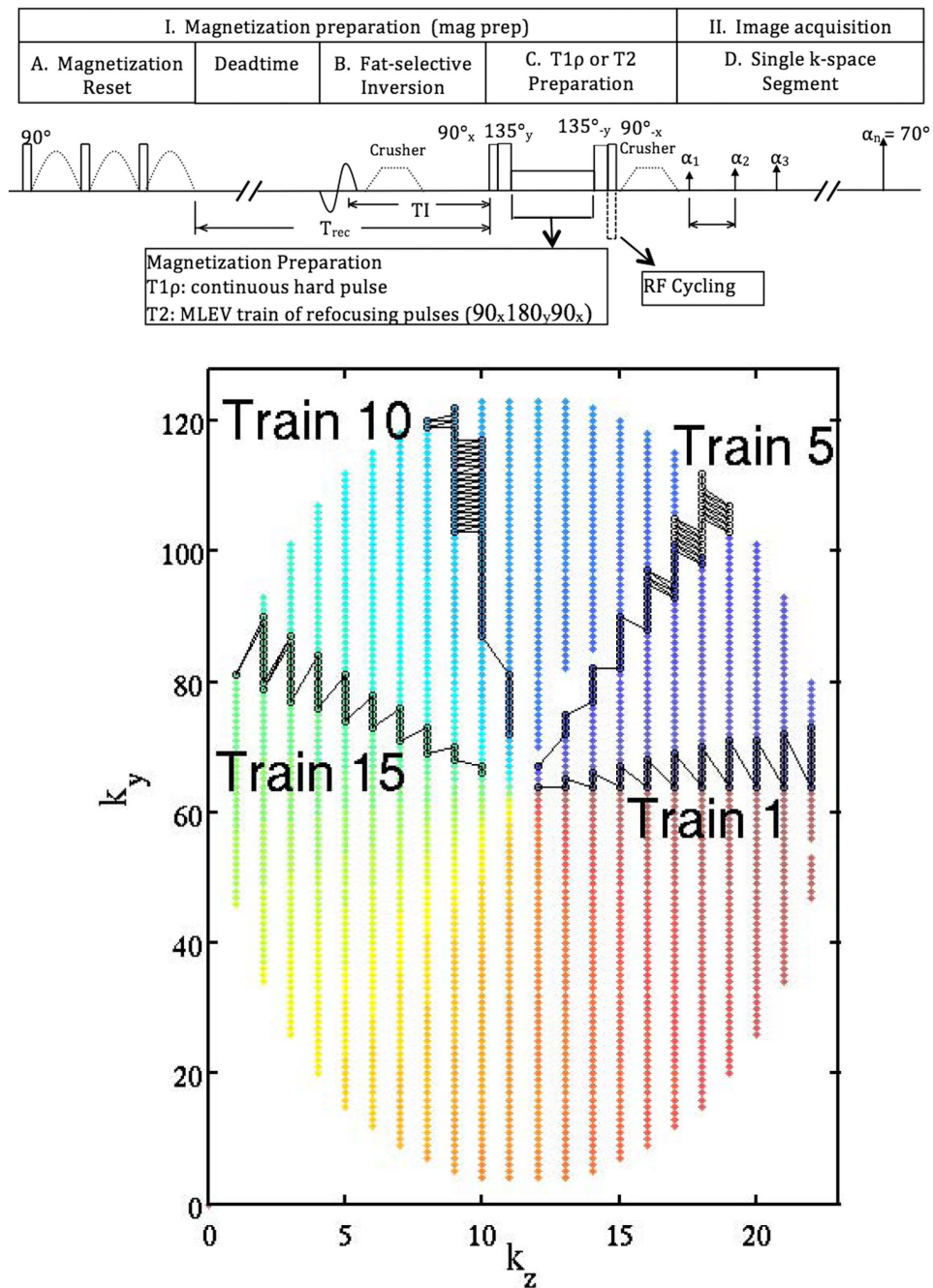


Figure 1.

(A) Pulse diagram of the combined $T_{1\rho}/T_2$ quantification based on the modified MAPSS sequence. Either the $T_{1\rho}$ or the T_2 preparation could be run for any echo, and the $T_{1\rho}$ - and T_2 -weighted images will be acquired in one scan sequence. Combining the composite pulses and RF-cycling can simultaneously correct B_0 magnetic field inhomogeneity effects and B_1 RF inhomogeneity effects. (B) The scheme of the k-space trajectory used in the sequence based on radial-centric view ordering.

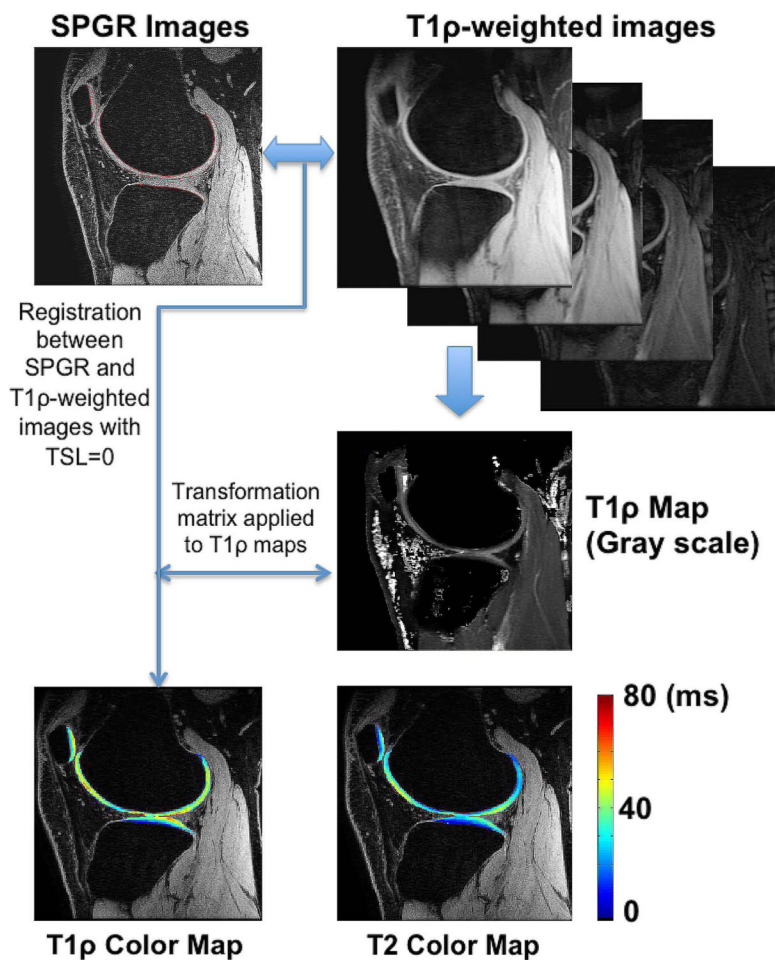


Figure 2. The diagram of image processing and quantification of the study. The cartilage was segmented on the high resolution SPGR images (red contours). T_{1 ρ} - weighted images with TSL = 0 were registered to SPGR using VTK registration toolkit. The registration transformation matrix was applied to the T_{1 ρ} or T₂ maps which were reconstructed from T_{1 ρ} - or T₂-weighted images. Example T_{1 ρ} and T₂ color maps overlaid on SPGR images are also shown.

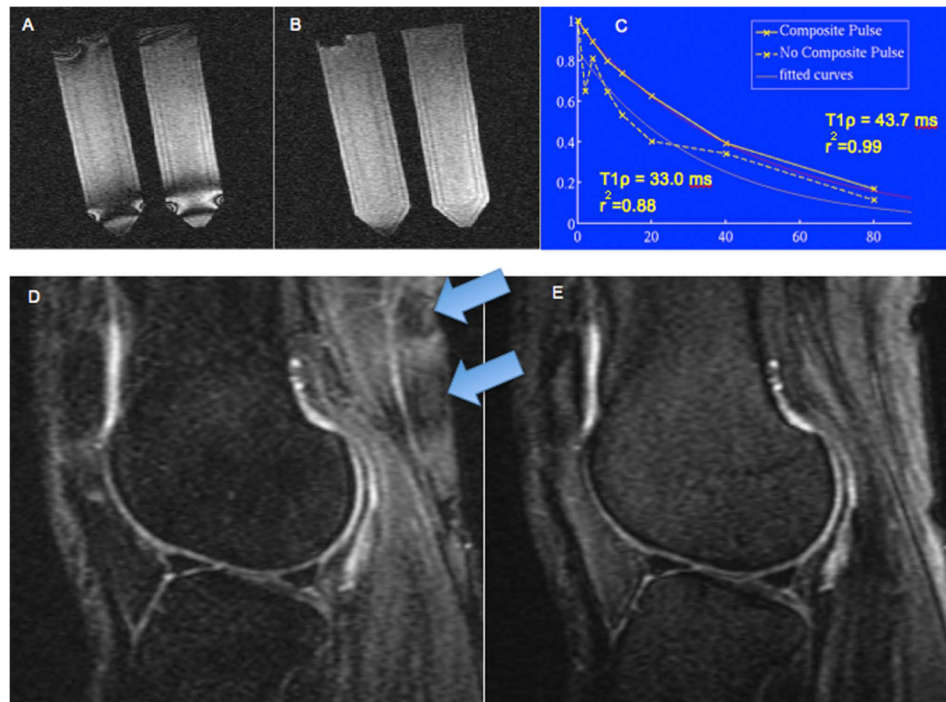


Figure 3.

$T_{1\rho}$ -weighted images of phantoms (time of spin-lock = 40 ms, spin-lock frequency = 500 Hz) and in vivo knees (lower row, time of spin-lock = 40 ms, spin-lock frequency = 500 Hz) with single 90 tip-down/tip-up pulses (A, D) and with composite tip-down/tip-up pulses (B, E) as shown in Figure 1. The banding artifacts (at the edge of the phantom, and indicated with blue arrows in the knee) were significantly reduced in images using composite pulses. The signal curve from the phantom (C) showed non-exponential signal oscillation in the data without composite pulses, which introduced a poor fitting and underestimate of $T_{1\rho}$ quantification; while the data using composite pulses had very good fitting of the exponential decay curve.

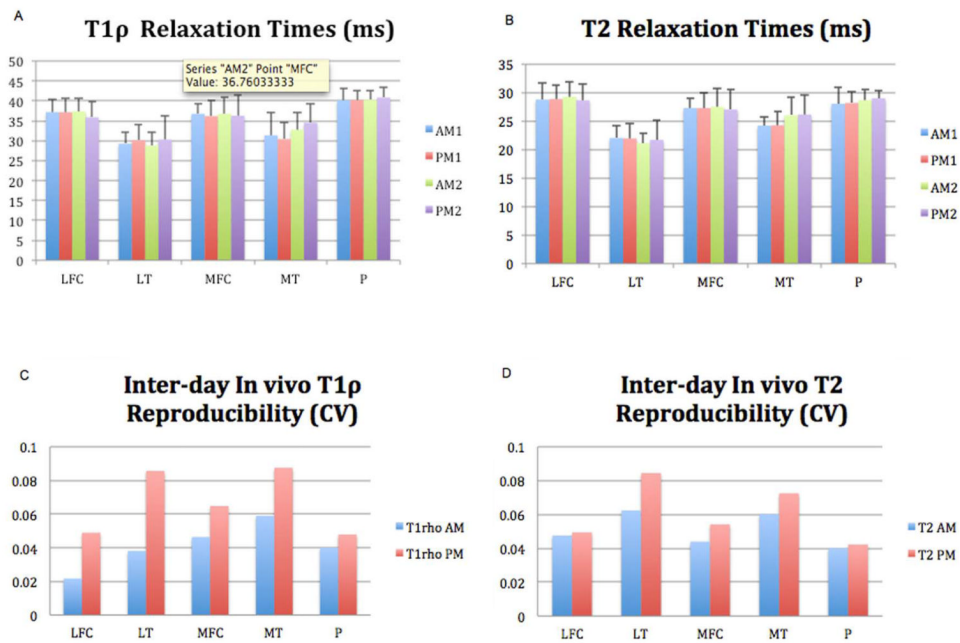


Figure 4. *In-vivo* T1 ρ (A) and T2 (B) quantifications of each defined compartments in each session, and the inter-day repeatability of T1 ρ (C) and T2 (D) quantifications. LFC: lateral femoral condyle; LT: lateral tibia; MFC: medial femoral condyle; MT: medial tibia; P: patella.

Table 1
Variation of T_{1ρ} and T₂ from morning to afternoon: (AM-PM)/AM×%

	LFC	LT	MFC	MT	Patella
T _{1ρ}	1.8%±5.6%	-3.4%±8.7%	1.2%±7.8%	-0.5%±14.8%	-0.3%±6.3%
T ₂	0.6%±7.4%	-1.2%±8.6%	1.0%±6.2%	-0.6%±8.1%	-0.1%±6.2%

L/MFC: lateral/medial femoral condyle; L/MT: lateral/medial tibia